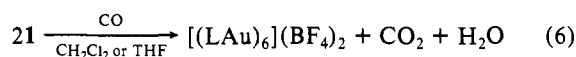
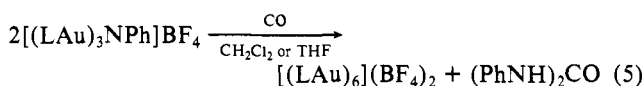


believed to derive from  $\text{H}_2\text{CO}_3$ , are formed from **1**.<sup>15</sup>



Solutions of **2** ( $\text{R} = \text{Ph}$ ), **3**, and **4** are much more stable than those of **2** ( $\text{R} = \text{Me}$ ), but they also decompose. The kinetics of these and other decompositions will be the subject of future studies directed at understanding the factors that determine the stability of the  $[(\text{LAu})_m\text{X}]^{n+}$  complexes.

**Acknowledgment.** We thank ARCO Chemical Company, the Division of Chemical Sciences, Office of Basic Energy Sciences, Office of Energy Research, U.S. Department of Energy (Grant No. DE-FG02-88ER13880) for support of this work, Dr. C. Barnes for assistance with the X-ray work, and the National Science Foundation for partial funding of the X-ray (CHE-9011804) and NMR (PCM-8115599) equipment.

**Supplementary Material Available:** Listings of kinetic data and details of the structure determinations (27 pages); tables of observed and calculated structure factors (33 pages). Ordering information is given on any current masthead page.

(14) The same results are obtained in MeOH, eliminating the possibility of free PhNCO involvement.

(15) Ureas were obtained in a related Rh system: see ref 1.

### Transition-State Structural Features for the Association of Metalloproteases with Phosphorus-Containing Inhibitors

Maria Izquierdo-Martin and Ross L. Stein\*

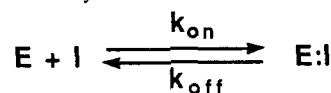
Department of Enzymology, R80N-A54  
Merck, Sharp, and Dohme Research Laboratories  
P.O. Box 2000, Rahway, New Jersey 07065

Received October 31, 1991

Many enzyme inhibitors reversibly combine with their targeted enzymes with second-order rate constants that are orders of magnitude lower than the diffusion limit.<sup>1</sup> In most cases, however, the reaction step that rate-limits these associations is unclear. We now report results of a study that probes the rate-limiting step for the association of the bacterial metalloprotease TLN<sup>2,3</sup> with phosphoramidon,<sup>4</sup> *N*-(( $\alpha$ -L-rhamnopyranosyloxy)hydroxyphosphinyl)-Leu-Trp (**1**), and the human matrix metalloprotease SLN<sup>5-7</sup> with the peptide phosphoramidate, phthalimido- $(\text{CH}_2)_4\text{P}(\text{O})(\text{O}^-)\text{-Ile-Nal-NHCH}_3$  (**2**).<sup>8</sup>

For both enzyme/inhibitor pairs, progress curves for substrate hydrolysis in the presence of inhibitor are characterized by an initial velocity,  $v_0$ , that slowly decays to the final, steady-state

**Scheme I.** Kinetic Mechanism for Slow-Binding Inhibition of Thermolysin and Stromelysin



velocity,  $v_s$ , with a first-order rate constant,  $k_{\text{obsd}}$ . Estimates of these three parameters were obtained by fitting the progress curves to the standard equation for slow-binding inhibition:<sup>1</sup>

$$[\text{product}] = v_s t + \left( \frac{v_0 - v_s}{k_{\text{obsd}}} \right) [1 - \exp(-k_{\text{obsd}} t)] \quad (1)$$

In both cases, the dependencies of  $v_0$ ,  $v_s$ , and  $k_{\text{obsd}}$  on inhibitor concentration are unexceptional (data not shown) and show that (i)  $v_0$  is independent of inhibitor concentration and equals the control velocity determined in the absence of inhibitor; (ii)  $v_s$  is dependent on inhibitor concentration according to eq 2; and (iii)  $k_{\text{obsd}}$  is linearly dependent on inhibitor concentration. These

$$v_s = \frac{v_0}{1 + \frac{[\text{I}]}{K_i}} \quad (2)$$

observations support the simple mechanism of Scheme I. According to this mechanism, the linear dependence of  $k_{\text{obsd}}$  on inhibitor concentration is described by eq 3. The dissociation constant,  $K_i$ , is therefore expressed as the simple relationship of eq 4. Note that these experiments were all conducted under the

$$k_{\text{obsd}} = k_{\text{on}}[\text{I}] + k_{\text{off}} \quad (3)$$

$$K_i = \frac{k_{\text{off}}}{k_{\text{on}}} \quad (4)$$

condition  $[\text{S}] \ll K_m$  (see footnote *a* of Table I for a description of the conditions). This allows us to use the substrate concentration independent eqs 2-4.

$K_i$ ,  $k_{\text{on}}$ , and  $k_{\text{off}}$  can be estimated from rearranged forms of eqs 2-4 as shown below:

$$K_i = \frac{[\text{I}]}{\frac{v_0}{v_s} - 1} \quad (5)$$

$$k_{\text{on}} = \frac{k_{\text{obsd}}}{[\text{I}] + K_i} \quad (6)$$

$$k_{\text{off}} = k_{\text{on}} K_i \quad (7)$$

In practice, a progress curve is analyzed according to eq 1 to obtain best-fit values for  $v_0$ ,  $v_s$ , and  $k_{\text{obsd}}$ .  $K_i$  is then calculated from eq 5 and used together with eq 6 to calculate  $k_{\text{on}}$ . Finally,  $k_{\text{off}}$  is estimated as  $k_{\text{on}} K_i$ . Table I summarizes values for these parameters.

To explore transition-state structural features for these reactions, we determined values of  $^{\text{D}}k_{\text{on}}$ , which, for both reactions, are large and normal (see Table I). For TLN and **1**, the proton inventory<sup>9,10</sup> for  $k_{\text{on}}$  was also determined and is "dome-shaped" (Figure 1). While several mechanisms can produce "dome-shaped" proton inventories,<sup>10-12</sup> previous studies with TLN<sup>13-15</sup> eliminate many

(1) Morrison, J. F.; Walsh, C. T. *Adv. Enzymol. Relat. Areas Mol. Biol.* **1988**, *61*, 201-301.

(2) Abbreviations: TLN, thermolysin; SLN, stromelysin; Nal, 3-( $\beta$ -naphthyl)-L-alanine; FA, 3-(2-furyl)acryloyl; DNP, 2,4-dinitrophenyl;  $^{\text{D}}k_{\text{on}}$ , solvent deuterium isotope effect on  $k_{\text{on}}$ ;  $^{\text{D}}k_{\text{off}}$ , solvent deuterium isotope effect on  $k_{\text{off}}$ ;  $^{\text{D}}K_{\text{assoc}}$ , solvent deuterium isotope effect on  $K_{\text{assoc}}$ .

(3) Morihara, K. *Annu. Rev. Biochem.* **1971**, *41*, 179-243.

(4) Kitagishi, K.; Hiromi, K. *J. Biochem.* **1984**, *95*, 529-534.

(5) Matrisian, L. M. *Trends Genet.* **1990**, *6*, 121-126.

(6) Harrison, R.; Teahan, J.; Stein, R. *Anal. Biochem.* **1989**, *180*, 110-113.

(7) Teahan, J.; Harrison, R.; Izquierdo, M.; Stein, R. L. *Biochemistry* **1989**, *28*, 8497-8501.

(8) **2** was designed and synthesized by Dr. Richard Galardy (University of Kentucky) as an inhibitor of human collagenase and was purchased from Elastin Products, Pacific, MO.

(9) Schowen, K. B.; Schowen, R. L. *Meth. Enzymol.* **1982**, *87*, 551-606.

(10) Quinn, D. M.; Sutton, L. D. In *Enzyme Mechanism Isotope Effects*; Cook, P. F., Ed.; CRC Press: Boston, 1991; pp 73-126.

(11) Stein, R. L.; Strimpler, A. M.; Hitoshi, H.; Powers, J. C. *Biochemistry* **1987**, *26*, 1305-1314.

(12) Stein, R. L. *J. Am. Chem. Soc.* **1985**, *107*, 6039-6043.

(13) Izquierdo-Martin, M.; Stein, R. L. *J. Am. Chem. Soc.* **1992**, *114*, 325-331.

(14) Izquierdo, M.; Stein, R. L. *J. Am. Chem. Soc.* **1990**, *112*, 6054-6062.

(15) Stein, R. L. *J. Am. Chem. Soc.* **1988**, *110*, 7907-7908.

**Table I.** Kinetic Parameters for the Slow-Binding Inhibition of Thermolysin and Stromelysin<sup>a</sup>

enzyme and inhibitor	$K_i^b$ (nM)	$k_{on}^b$ ( $\text{mM}^{-1} \text{s}^{-1}$ )	$k_{off}^b$ ( $10^{-5} \text{s}^{-1}$ )	$^D k_{on}^c$	$^D K_{assoc}^d$	$^D k_{off}^e$
TLN + 1	$0.4 \pm 0.1$	$110 \pm 12$	$4 \pm 1$	$1.70 \pm 0.05$	$0.65 \pm 0.08$	$2.6 \pm 0.3$
SLN + 2	$23 \pm 3$	$9.8 \pm 0.3$	$25 \pm 14$	$1.51 \pm 0.11$		

<sup>a</sup> These parameters were determined from inhibition progress curves (see text). For TLN, hydrolysis of FA-Gly-LeuNH<sub>2</sub> was followed spectrophotometrically at 345 nm. In a typical experiment (pH 5.5, 25 °C), [E]<sub>0</sub> = 10 nM, [S]<sub>0</sub> = 2 mM, and [I]<sub>0</sub> = 20 nM. All reagents were purchased from Sigma Chemical Co. For SLN, hydrolysis of DNP-Arg-Pro-Lys-Pro-Leu-Ala-Phe-TrpNH<sub>2</sub> was monitored as a change in fluorescence intensity ( $\lambda_{ex}$  = 280 nm,  $\lambda_{em}$  = 340 nm). In a typical experiment (pH 6.0, 25 °C), [E]<sub>0</sub> = 15 nM, [S]<sub>0</sub> = 10  $\mu\text{M}$ , and [I]<sub>0</sub> = 0.5  $\mu\text{M}$ . SLN was a gift of Dr. M. Lark; substrate was prepared by Bachem; and **2** was purchased from Elastin Products. This is a new assay (cleavage at Ala-Phe,  $k_c/K_m$  = 43  $\text{mM}^{-1} \text{s}^{-1}$ ; details to be published later) and is based on the release of internal quenching of Trp by DNP that occurs as the two hydrolysis products diffuse apart in solution.<sup>23,24</sup> <sup>b</sup> See text for details of analysis. <sup>c</sup>  $^D k_{on}$  is the mean and standard deviation for the combined results of three independent isotope effect experiments. Each of these experiments involved no fewer than four individual isotope effect measurements, where each isotope effect measurement is the ratio of two kinetic runs:  $k_{on,H_2O}/k_{on,D_2O}$ . Values of  $k_{on}$  were calculated as described in the text. <sup>d</sup> Solvent deuterium isotope effect on  $K_{assoc}$ , where  $K_{assoc} = 1/K_i$ . Values of  $K_i$  were calculated as described in the text. <sup>e</sup>  $^D k_{off} = ^D K_{assoc}/^D k_{on}$ .

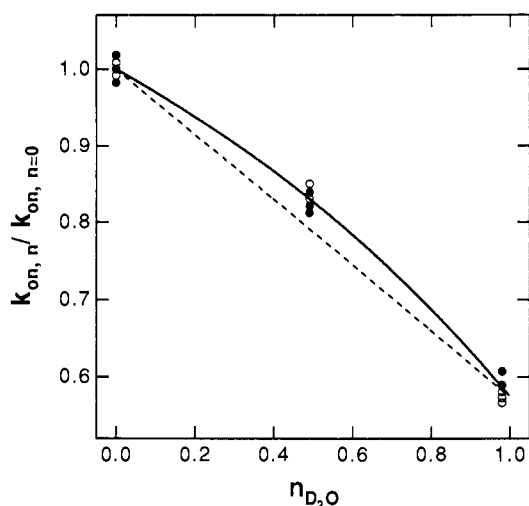


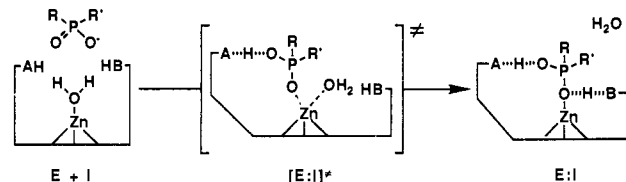
**Figure 1.** Proton inventory for  $k_{on}$  for the inhibition of TLN by **1**. To increase the precision of our determinations of  $k_{on}$ , we set **1** equal to 20 nM. At this concentration,  $k_{on}[I] = (10^5 \text{ M}^{-1} \text{ s}^{-1})(20 \text{ nM}) = 200 \times 10^{-5} \text{ s}^{-1} \gg k_{off} = 4 \times 10^{-5} \text{ s}^{-1}$ . Therefore,  $k_{obsd} = k_{on}[I]$  with no contribution from  $k_{off}$ . The data from two independent experiments are shown. The solid line was drawn using eq 8 and the best-fit fractionation factors given (see text). The dashed line was included to emphasize the curvature of the best-fit line.

of these and favor interpretation of Figure 1 in the context of eq 8, where the apparent isotope effect at mole fraction solvent

$$\frac{k_n}{k_{n=0}} = \frac{1 - n + n\phi_{\ddagger}}{(1 - n + n\phi_R)^2} \quad (8)$$

deuterium,  $n$ , is expressed as a function of  $\phi_{\ddagger}$ , the fractionation factor for the isotope-effect-generating proton in the transition state, and  $\phi_R$ , the fractionation factor for one of two protons in the reactant state that contributes to the observed isotope effect. The data of Figure 1 were fit to eq 1 to yield  $\phi_{\ddagger} = 0.417 \pm 0.028$  and  $\phi_R = 0.852 \pm 0.026$ . Thus, the observed isotope effect of 1.74, calculated from eq 8 with  $n = 1$ , originates from a transition-state contribution,  $\phi_{\ddagger}^{-1}$ , of 2.4 diminished by a reactant state contribution,  $\phi_R^2$ , of 0.73.

From the proton inventory, three points emerge: (i) The reactant-state term agrees with estimates of  $\phi_R$  that have previously been determined for reactions of TLN<sup>13-15</sup> and is similar to  $^D K_{assoc}$  (Table I), which is a measure of  $\phi_R^2$ .<sup>13</sup> This term reflects the two protons of the catalytically essential zinc-bound water.<sup>3,16-20</sup> (ii) The transition-state term suggests the existence of a stabilizing protonic bridge (or bridges) of the sort that is observed in general-acid/general-base catalysis.<sup>10</sup> (iii) The ability of eq 8 to

**Scheme II.** Proposed Transition-State Structure for the Interaction of Phosphorus-Containing Inhibitors with Metalloproteases

account for the data of Figure 1 suggests that the transition-state contribution originates at a single protonic site. Simulations of proton inventories indicate that if the transition-state term originated at more than a single protonic site, the proton inventory would be linear or "bowl-shaped".

These results together with the normal isotope effect on  $k_{on}$  for the association SLN and **2** allow us to eliminate two mechanisms that could possibly account for slow E:I formation: a rate-limiting enzyme conformational change and "rare form" inhibition. The former is eliminated since protein conformational changes are unlikely to produce large solvent isotope effects or, if they do, these effects are anticipated to originate at many protonic sites.<sup>10-12</sup>

We also rule out mechanisms in which the inhibitor reacts at the diffusion limit with a thermodynamically "rare" form of the enzyme. In such cases, transition-state fractionation factors will be unity and the isotope effect will originate from reactant-state contributions alone. If such a mechanism obtained for TLN, as suggested,<sup>21</sup>  $^D k_{on}$  would have been inverse and near 0.75.

Our results suggest that  $k_{on}$  is rate-limited by some chemical step that is subject to protolytic catalysis. We propose that this step is ligand exchange of the inhibitor for the zinc-bound water molecule. One possible depiction of this process and its transition state is shown in Scheme II. According to this mechanism, formation of E:I is accompanied by displacement of zinc-bound water to bulk solvent and formation of two hydrogen bonds between inhibitor and active-site residues. This hypothesis is consistent with the known structure of TLN:**1**<sup>22</sup> and readily forms a mechanistic framework for interpretation of our isotope effect data. In [E:I]<sup>‡</sup>, displacement of zinc-bound water is accompanied by formation of a catalytic proton bridge of the sort described by Kreevoy.<sup>25</sup> Proton bridges of this sort form during protolytic catalysis<sup>10</sup> and manifest fractionation factors that are less than unity. Fractionation factors for the protons of the departing water molecule should be near unity in [E:I]<sup>‡</sup> since the influence of the zinc will be diminished relative to the reactant state where  $\phi_R$  equals 0.85. Finally, the hydrogens in E:I and the released water will all have fractionation factors of unity. This mechanistic proposal is supported by our observation of large, normal solvent isotope effects on both  $k_{on}$  and  $k_{off}$ .

(16) Hanguer, D. G.; Monzingo, A. F.; Matthews, B. W. *Biochemistry* **1984**, *23*, 5730-5741.

(17) Holmes, M. A.; Matthews, B. W. *Biochemistry* **1981**, *20*, 6912-6920.

(18) Holmquist, B.; Vallee, B. L. *Biochemistry* **1976**, *15*, 101-107.

(19) Kester, W. R.; Matthews, B. W. *Biochemistry* **1977**, *16*, 2506-2516.

(20) Monzingo, A. F.; Matthews, B. W. *Biochemistry* **1984**, *23*, 5724-5729.

(21) Bartlett, P. A.; Marlowe, C. K. *Biochemistry* **1987**, *26*, 8553-8561.

(22) Weaver, L. H.; Kester, W. R.; Matthews, B. W. *J. Mol. Biol.* **1977**, *114*, 119-132.

(23) Netzel-Arnett, S.; Mallya, S. K.; Nagase, H.; Birkedal-Hansen, H.; Van Wart, H. E. *Anal. Biochem.* **1991**, *195*, 86-92.

(24) Stack, M. S.; Gray, R. D. *J. Biol. Chem.* **1989**, *264*, 4277-4289.

(25) Kreevoy, M. M.; Liang, T.; Chang, K. C. *J. Am. Chem. Soc.* **1977**, *99*, 5207-5209.